p-ISSN 2089 – 0133 e-ISSN 2477-6416
URL : https://jurnal.uns.ac.id/ijap/article/view/93092
Indonesian Journal of Applied Physics (IJAP) Vol. 14 No. 2 page 386
DOI : https://doi.org/10.13057/ijap.v14i2.93092

MONTE CARLO SIMULATION AS PRECISION PREDICTIVE TOOLS TO FIND ISODOSE CURVE OF GAMMA IRRADIATOR: A PRELIMINARY STUDY

Bimo Saputro*[1,2], Adhi Harmoko Saputro[1], Nunung Nuraeni[2], Heru Prasetio[2], Okky Agassy Firmansyah[2], Fendinugroho[2], Hasan Mayditia[2]
[1]Faculty of Mathematics and Natural Sciences, University of Indonesia, Depok, Indonesia
[2]National Research and Innovation Agency, Serpong, Tangerang Selatan, Indonesia
*bimo001@brin.go.id

Received 05-09-2024, Revised 12-10-2024, Accepted 20-10-2024,
Available Online 20-10-2024, Published Regularly October 2024

ABSTRACT

Dose distribution mapping is critical for guaranteeing correct sample irradiation, with both experimental and simulation methods playing important roles. Simulations are an effective way to forecast dose distribution patterns, lowering costs and increasing resource utilization. The geometry, source configuration, and measurement locations are fundamental to determine. The gamma irradiator has 48 source areas, each containing two cobalt-60 pencils measuring 8.15 cm, as well as a 4.7 cm stainless steel dummy. Alanine dosimeters were used for dose assessments, and stability varied by less than 1% over six months at 6°C and up to 5% at 50°C. The study's findings revealed a 2.25% disparity in relative dosage between experimental measurements and PHITS models. This result is major improvement over prior research that found a 10% difference. Furthermore, dosage mapping along the XY and Z axes revealed the most uniform zone on the Z-axis, measuring 7.5 cm to 12.5 cm with a radius of no more than 5 cm. The study implies that this model can be used to improve the arrangement of cobalt-60 pencils in the irradiator, improving homogeneity and radiation outcomes.

Keywords: Dose distribution; experimental; gamma irradiator; simulation.

Cite this as: Saputro, B., Saputro, A. H., Nuraeni, N., Prasetio, H., Firmansyah, O. A., Fendinugroho., & Mayditia, H. 2024. Monte Carlo Simulation as Precision Predictive Tools to Find Isodose Curve of Gamma Irradiator: A Preliminary Study. *IJAP: Indonesian Journal of Applied Physics, 14*(2), 386-398. doi: https://doi.org/10.13057/ijap.v14i2.93092

INTRODUCTION

A gamma irradiator is an essential component in radiation processing. It consists of three important elements: a Cobalt-60 source, a product container, and a product irradiation path. All of these factors influence the distribution of radiation dose in the irradiation room, which, in turn, affects the accuracy of the dose obtained by the target product. The uniformity of dose distribution within the irradiation chamber is critical, but it becomes more difficult in varied-dimension chambers, which might result in a heterogeneous total dosage distribution [1]. Dose distribution is significantly influenced by several factors such as the arrangement of Cobalt-60 source pencils, the arrangement of source racks with the irradiated product, the dimension of the irradiation chamber [2]. Dose distribution mapping is an important method for ensuring that irradiated samples receive the correct dose. It also contributes to the Dose Uniformity Ratio (DUR), which reflects the range between the maximum and minimum doses [3]. The key instrument for validating and simulating doses in irradiators is required to ensure the success

of treatments. Improving precise measurement in areas such as dosimetry involves the adoption of low-cost, easy-to-apply methods [4]. Experiments, including the placement of dosimeters at various positions within the irradiation chamber, can contribute to measurement [5]. Another way for validation is to utilize simulation software to determine and compare the measured radiation dosage received by the dosimeters [6]. Backscatter and field radiation size can have an impact on dosimeter utilization for a variety of reasons [7]. Validation measures using simulation code can involve comparing dosimeter measurements to simulation findings. A decent agreement between two different types of measurements is greater than 10% [8]. Table 1 explains the comparison of studies on Monte Carlo-based irradiators.

Table 1. Comparative Study on Irradiator Using Monte Carlo [9]

Facility	Year	Software	Dosimeter	Relative Dose Difference
Bangladesh	2018	MCNPX 2.7	Fricke and Cerric-cerrous	Max 12 %
Brazil, GB-127	2017	MCNPX	Fricke	Max 8 %
MDS Nordion	2019	MCNPX 2.9	Fricke	Max 21%
Croatia, Technabsexport	2019	Geant4	Ion Chamber	Max 6 %
USSR (Rusia)	2024	PHITS	Ion Chamber, ECB	Max 5.0 %
Morocco, Co-60	2020	MCNPX	Alanine	Max 7.3 %
	2020	MCNPX	Fricke	Max 9.0 %
	2021	MCNPX	Alanine	Max 9.0 %
	2023	Geant4	Fricke	Max 9.0 %
France	2022	MCNPX 2.7, RayXpert software	Alanine	2.4 % dan 4.1 %

According to Table 1, there was a 5% relative dose difference in previous research using PHITS software. The table also indicates that a 2.4% relative dose difference can be attained. It is possible to use innovation and opportunities to get a relative dose differential on PHITS software that is less than 5%. This accomplishment will be on par with or better than the ones made using the MCNPX 2.7 software. Simulation methods offer an efficient approach to analyzing dose distribution patterns before conducting experiments, resulting in cost reduction and improved resource utilization. By leveraging software-based simulations, researchers can determine isodose curves and gain valuable insights into expected dose distribution patterns [10]. This allows for informed decision-making and optimization of the gamma irradiation process. Furthermore, simulations help to identify potential flaws and adopt remedial actions, ultimately enhancing the quality and efficiency of radiation-based applications [11]. Samples/products being irradiated inside the source rack require knowledge of the dose rate, irradiation settings, and irradiation time computation. An accurate and precise dosimetry measurement is crucial for filling gaps in the irradiation treatment (reaching the minimum absorbed dosage, not exceeding the maximum dose, and ensuring a uniform dose distribution within the sample). In some circumstances, both measurements and MC simulation computations are required to compare the result. MC simulation will help with the best irradiation strategy and compute the dose for complex samples and/or areas where measurements are not possible [12]. These studies fill the gap related to the accuracy of

dosimeter measurements on multi-source cobalt-60 gamma irradiator. This study aims to compare dosimeter measurements and Monte Carlo simulations using PHITS on Gamma Cell 220 and get a relative dose difference of less than 5%. The findings of this work contribute to the progress of dose distribution techniques and the optimization of gamma irradiation processes. The offered methodologies and indicated study areas advance the field, boosting the quality and efficiency of radiation-based applications.

METHOD

Gamma Cell 220

Gamma Cell 220 is a category-one gamma irradiator manufactured by CANADA in 1968. Category one irradiator is a dry storage irradiator with a stationary radioactive source while moving products. The dimensions of the irradiation chamber are Ø15 cm with a height of 20 cm [12]. Figure 1 shows the Gamma Cell irradiator source configuration. The yellow color has the same activity for each 713 Ci, the blue color for each 1406 Ci, and the green color for each 989 Ci. Meanwhile, the gray color is a dummy source of a solid iron casing.

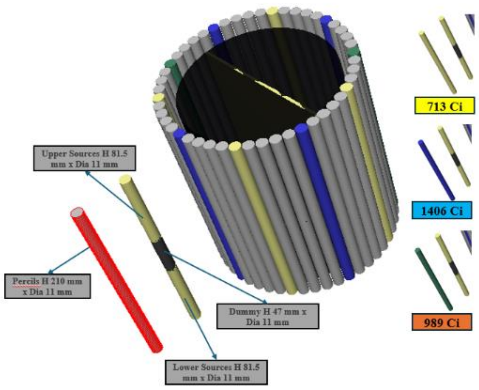

Figure 1. Source Configuration on Gamma Cell 220

Details of the source activities are described in Table 2. Four other types of pencil sources with the same source activity (Figure 1. shows yellow colors). Two types of pencil sources with the same source activity (Figure 1. shows green colors). Gamma Cell 220 irradiator designed with a maximum Co-60 source capacity is 12 kCi. The capacity of the source pencils is 48 source spaces and contains ten spaces. In one pencil source, there are two cobalt 60 measuring 8.15 cm and a solid stainless steel dummy measuring 4.7 cm, so the length of one pencil source is ^{21} cm [13]. Each source assembly consists of a stainless steel cylindrical holder carrying four 60Co source pencils, which are closed by a protective plug [9].

Mapping the distribution of radiation at radioactive sources requires a measuring instrument called a dosimeter. Dosimetry methods for measuring dose rate distribution in the irradiation chamber include red Perspex (dose range: 5-50 kGy), amber Perspex (dose range: 1-15 kGy), and cellulose triacetate (dose range: 0.1-100 kGy), alanine (dose range: 20 Gy to 80 kGy). The absorbed dose rate is then calibrated to the Alanine/EPR as a reference dosimetry system. Uncertainties of measurements shall follow the ISO/ASTM Standard (ISO/ASTM, 2015) [14].

Table 2. Summary of Gamma Cell 220 Technical Specification

Position Source	Source Number	INITIAL		Source Number	INITIAL	
	Lower	Activity (Bq)	Activity (Ci)	Upper	Activity (Bq)	Activity (Ci)
1	K158	3.89E+13	1050.3	K181	1.32E+13	356.67
6	K180	1.32E+13	356.67	K184	1.32E+13	356.67
10	K166	2.34E+13	632.34	K175	1.32E+13	356.67
15	K182	1.32E+13	356.67	K156	3.89E+13	1050.3
20	K173	1.32E+13	356.67	K174	1.32E+13	356.67
25	K155	3.89E+13	1050.3	K186	1.32E+13	356.67
30	K177	1.32E+13	356.67	K165	2.34E+13	632.34
34	K176	1.32E+13	356.67	K178	1.32E+13	356.67
39	K183	1.32E+13	356.67	K157	3.89E+13	1050.3
44	K179	1.32E+13	356.67	K187	1.32E+13	356.67

Monte Carlo: PHITS

The Monte Carlo approach is widely utilized in a variety of disciplines, including physics, engineering, economics, computer science, and others. Its applications include option pricing in finance, radiation transport models in physics, optimization challenges, and risk analysis. The Monte Carlo method's strength is its ability to deal with complicated systems that contain various variables and uncertainties. By periodically choosing and analyzing random configurations, it gives a probabilistic understanding of the system's behavior, allowing for decision-making and problem-solving in situations when deterministic solutions are not possible. The Monte Carlo method is a precise scanning methodology for simulating the physical circumstances of energy transport and deposition processes. This approach is a theoretical reference in solutions with ionizing and non-ionizing radiation [15]. This technique is also efficient and adaptable for simulating photon-matter interactions as well as the real conditions of each experimental state. The benefit of the Monte Carlo approach can be to calculate absorbed doses in different materials of irradiated goods with variable geometries and densities. This method can handle difficult problems [16]. Figure 2 illustrates the movement of particles in water medium in PHITS software.

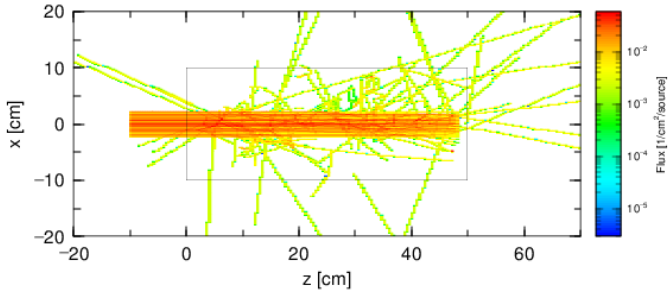

Figure 2. PHITS image from particle fluence around a cylindrical water tank irradiated by a 290-MeV proton beam [17].

The Particle and Heavy Ion Transport Code System (PHITS) is a simulation system developed by the Japan Atomic Energy Agency, the Research Organisation for Information Science and Technology, the High Energy Accelerator Research Organisation, and several other organizations. This program can compute the reaction and movement of the number of particles. The EGS5 method was used on the particles to transport electrons, positrons, and

photons. PHITS can simulate detector or dosimeter response by identifying the detector geometry and using actual detector or dosimeter components. Aside from that, simulation can evaluate the efficiency of dose distribution direction and visualize three-dimensional absorb dose distribution during irradiation [18]. Figure 5 shows a dimensional 3D image in PHITS. Where 3D dimensional images can be drawn directly on the XYZ axis in the PHITS software. Axis also shows the size and dimensions of space.

Experimental Setup

Reference dosimeters, also known as secondary standards, are accurate and reliable and calibrated using a primary standard. This category includes chlorobenzene ethanol, alanine, and Fricke dosimeters, among others. Most reference dosimeters can also be used to correlate a less accurate to a higher precision dosimeter, such as a primary standard dosimeter, so forming a link in the calibration chain ensures the system's traceability. Such dosimeters are known as transfer dosimeters [19]. Current alanine dosimetry relies on a calibration curve derived from irradiating dosimeters with a Co-60 beam. The absorbed dose of water is traceable to primary standards. Traceability is very important to ensure the true value of measurement [20]. Alanine dosimeter is a measuring instrument in the dosimetry system that can be corrected using temperature. Production of free radicals from the alanine dosimeter is not only affected by changes in the mass energy absorption coefficient but also due by an intrinsic decrease in free radical production per dose. The energy-dependent effect of free radical production will be more pronounced if the radicals are generated from low-energy photons [21]. Figure 3 explains the alanine spectrum model in the Electron Spin Resonance (EPR) device.

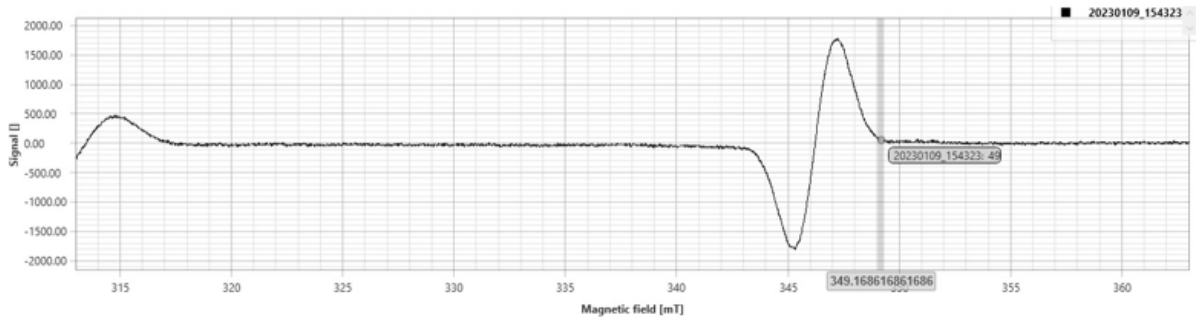

Figure 3. EPR spectrum of irradiated alanine dosimeter. Resonance peaks between 325 mT and 340 mT are contains free-redicals. Resonance peak at 350 mT corresponds to the spectrometer's internal ruby reference.

Alanine dosimeters are very stable under different conditions, including dose, dose rate, energy, temperature, humidity, and light. Alanine can produce a stable signal on ESR and only produces a difference of 1% for six months stored at 6 degrees Celsius and up to a maximum of 5% stored at 50 degrees Celsius. Humidity affects only 5%. The average dosimeter response was about 0.7% over an 11-month period when stored in a desiccator and 14% when stored at room conditions [22]. Figure 3 explains the measuring position of the dose deposit at the central irradiation chamber (height 10 cm from the bottom, radius 7.5 cm).

Figure 4. Dose deposit measurement at central position of chamber

The purpose mapping at the center point determines the absolute dose value. An alanine measuring equipment (dosimeter) is used to take measurements. The absolute dose will be compared to the dose deposited in the PHITS Monte Carlo calculation to obtain the relative difference. The relative difference between experimentally observed (EXP) and computed (PHITS) values, denoted as (D'exp - D'PHITS)/D'exp), varies at a specific value [9]. The relative difference describes the appropriateness value of the Monte Carlo modeling; the closer it is to the true value, the closer the modeling is correct. To assess the difference between computed and measured values, we use a term called relative dose difference (RDD) [14]. The relative dose difference (RDD) is an important metric in radiation dosimetry that compares the accuracy of dose distributions predicted by computational models (such as Monte Carlo simulations) to experimentally obtained data. It gives a normalized comparison, making it easier to examine the differences between expected and observed doses. In mathematics, the RDD at a certain position in the target volume is defined as the ratio of the difference between the Monte Carlo computed dose (Dmc) and the measured dosage (Dmeasured), relative to the measured dose.

$$\text{Relative Dose Difference (RDD)} = \frac{Dmc - Dmeasured}{Dmeasureed} \times 100\%$$

This formula returns a percent value that represents the size of the simulated dose's divergence from the measured dose, normalized to the measured dose itself. An RDD result near 0 shows good agreement between simulation and measurement, meaning that the Monte Carlo model accurately depicts the dose distribution in the defined spatial region. Each prepared lot of dosimeters was submitted to the reference laboratory, Riso High Dose Reference Laboratory-HDRL-DTU Nutech in Denmark, to be irradiated with various radiation doses (as per the CIRM 2009 NPL Document) [23]. Four separate dosimeters were sent for each of the doses listed. A calibration curve was created using these reference dosimeters and used to compute the irradiation response dosage [24]. The alanine setup was carried out vertically in a 7.5 cm radius of the chamber. Alanine blisters are arranged in 15 dose points at 1.3 cm intervals. The radiation results are read based on the calibration curve traced at the Secondary Standard Dose Laboratory RISO Denmark. Calibration capability is defined at the Gamma source and in the range of 100 Gy to 100 kGy [22].

RESULT AND DISCUSSION

Dose Comparison Measurement and Simulations

The result indicates a change in dose value at the same location (see Figure 4. Position 10 cm from the bottom), and a total of sixteen doses were tested. Then, the alanine measurement

dosage was compared to the deposit dose in the PHITS simulation. Table 3 shows the relative dose difference values between measurements and simulations.

Table 3. Dose comparison at fixed radius and certain Z axes positions

No	Dose Alanine (Gy)	Dose PHITS (Gy)	RDD
1	116	114.5	-1.30%
2	174	174.2	0.10%
3	264	265.5	0.60%
4	400	404.6	1.10%
5	603	616.6	2.30%
6	918	939.7	2.40%
7	1390	1432.2	3.00%
8	2120	2182.8	3.00%
9	3220	3326.7	3.30%
10	4930	5070.6	2.90%
11	7580	7727.6	1.90%
12	11500	11777.7	2.40%
13	17500	17949.4	2.60%
14	26700	27356.9	2.50%
15	40900	41693.6	1.90%
16	63000	63543.9	0.90%

The smallest relative dose difference (measurement and simulation) is 0.10%, while the highest is 3.30%. The average standard error across all target doses is 1.85%. However, in a typical research irradiator with a stationary source, the overdose ratio can be approximately 10%; by comparison, the detected overdose ratio is tolerable. Although the variations did not follow a linear relationship, they will diminish with improved dosimeter accuracy and Monte Carlo history[25]. The simulation findings were in excellent agreement with the experimental data, with an average relative difference of less than 5%, according to the prior result from Jecong et al. 2022 [26]. Additionally, there was a minor difference in the average dosage rate between the two approaches. The small discrepancies result from the small number of dosimeters and their slightly inaccurate placement at crucial points throughout the measurement [26]. It might also be caused by the uncertainty surrounding the activity of the five sources and some estimates made during the irradiator modelling [26]. The results are displayed in Table 3, where the target absorbed dosage applied determines the relative dose difference range. Therefore, more research into the precision position and accuracy of the uncertainty measurement is required. The linearity curve yielded a 2.25% relative dosage discrepancy between measurement and simulation. Table 4 presents the results of the dose rate comparison.

Table 4. Relative Difference Between PHITS (simulations) and Alanine (measurement).

Items	Dose per hour	Dose per second
Dose PHITS	4739.0 Gy/hour	1.32 Gy/s
Dose Alanine	4634.9 Gy/hour	1.29 Gy/s
Relative Dose Difference		2.25%

The dose rate is obtained by plotting the curve between dose (Y axes) and time of irradiation (X axes). The dose rate is defined as the dose rate per unit of time. This method will obtain a comparison of relative dose differences on all target doses (measurement and Monte Carlo) used. A difference of less than 9% was used to indicate that the geometry simulation, source definition, and dose rate calculation technique were satisfactory. This dosage rate difference is

acceptable because it compares all measurements obtained using both methods [27]. According to an earlier study (table 1), if the relative dose difference is less than 10%, the simulation findings are close to reality (experimental settings). The simulation's veracity should be evaluated to guarantee that the simulation-based irradiation space mapping is accurate.

Gamma Particle Distributions in Simulations

Dose distribution mapping is performed at the radial position of the X and Y axes to assess the degree of radiation homogeneity at that location. Figure 5 shows the radiation dispersion along the X and Y axes. The goal of characterizing dose inhomogeneities in the sample chamber is to build a holder that will provide a spot with homogeneity regions at the irradiator center [28].

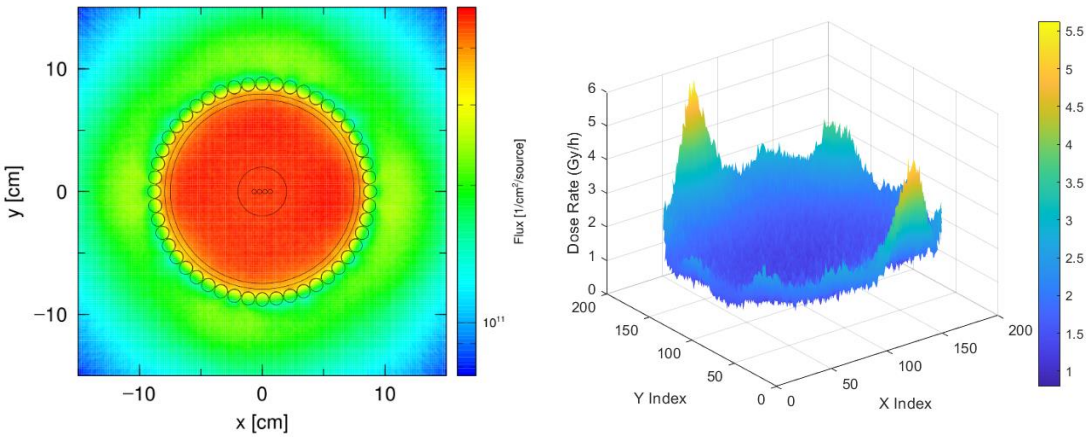

Figure 5. Dose distribution at a height of 10 from the bottom chamber along XY axes with diameters of 15cm.

Each little cube (voxel) on the irradiation position has a varied average photon energy depending on the distance from sources. The inner row's middle chamber is where the average energy is most homogeneous. The ratio of the maximum to the least average dose rates in the irradiation chamber is known as the dose uniformity in a specific box [29]. An isodose curve is formed by connected dose points, and a dosage distribution trend is formed by the isodose's overall distribution. The most homogenous areas of the irradiation chamber can be found using the dose distribution in a direction (XY) [30].

The vertical radiation distribution is measured to determine the radiation dispersion throughout the space. According to Figure 1, the radioactive source measures 81.5 mm, whereas the dummy (solid iron) measures 47 mm in a 210 mm long wrapping sleeve. The dummy is in the center of the sleeve, surrounded by two radioactive sources. This condition is present in all (10 sleeves) configured sources. Figure 6 shows the radiation dispersion in the radius and overall vertical position.

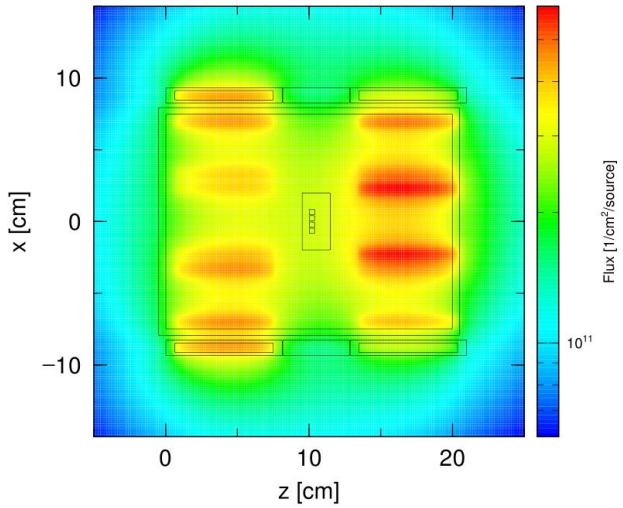

Figure 6. Dose distribution at vertical plane (Z axes) outside the irradiation chamber.

Many additional operating irradiators with various source–product configurations have real efficiency results that are in good agreement with the estimated values derived using the established approach. There are 1-3% differences between the estimated and actual efficiency. In the future, it may be possible to investigate the viability of irradiating a low- or high-dose product by altering the plant's source strength. However, the measurement evaluation in detail cannot account for the homogeneity in the irradiation chamber; so, Monte Carlo was used to finish this project [31]. Figure 7 shows that the longer the sampling radius from the vertical axis (Z axis), the greater the inhomogeneity. This is especially true if flat dose areas within the Gamma Cell 220 irradiation chamber are used effectively. The vertical distribution with several sample sections is displayed in Figure 7, ranging in radius from 0.5 cm to 7.5 cm. The data indicates that the sample is less homogeneous if the radius is larger. The sample is going closer to the radiation source with various kinds and activities, which is probably the case problem. Then it is possible to determine from this data that a more homogeneous and even distribution of the target item can only be obtained with a smaller sample volume. Furthermore, the dose maps may provide a suitable irradiation location for any thin sample with a changing surface area to produce a homogeneity dose at the region [26]. Figure 7 shows the results of vertical axis inhomogeneity at a specific sample radius.

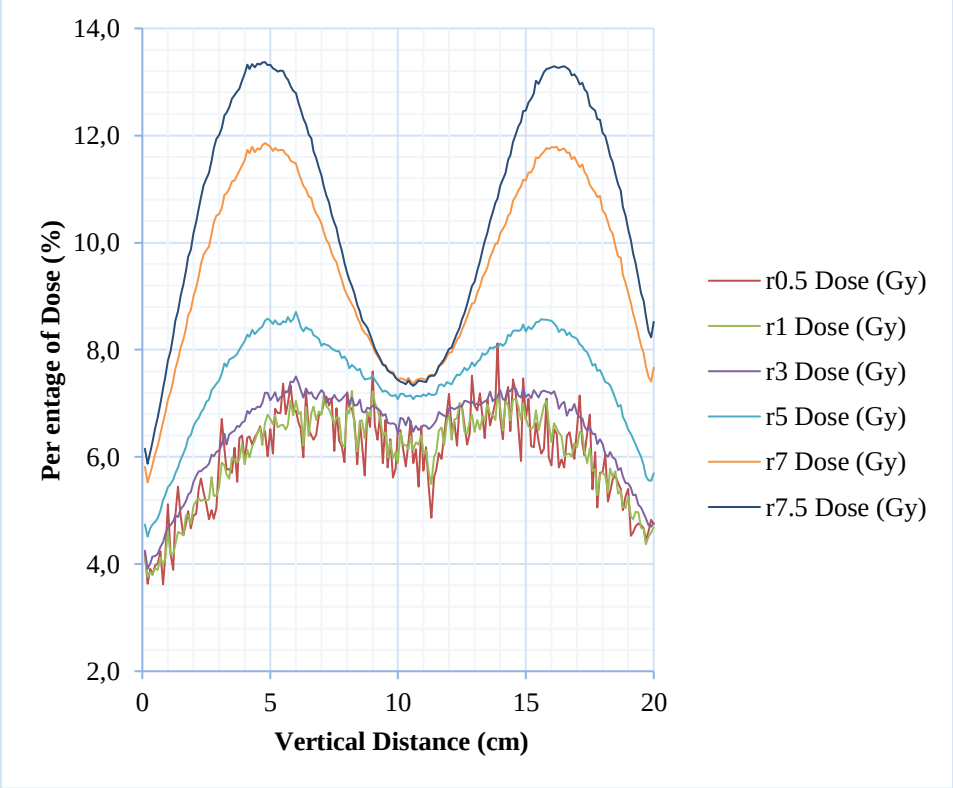

Figure 7. Dose uniformity in vertical chamber (Z axes)

Change the sampling radius to take measurements on the chamber's vertical axis. The bigger the sampling radius, the closer the data will be to homogeneity. This scenario happens because the radiation source in the casing has an inhomogeneous configuration. The dose in the top and bottom regions is slightly higher than the middle region because the total activities of the topmost and lowest sources are slightly higher than the middle, in this case only a dummy (solid iron). The simulation results are found to be in excellent agreement with the experimental results, with an average relative difference of 2.25%, which is better than the previous experiment conducted by Jecong et al. at the Philippine Nuclear Research Institute using MCNP5 annular ring voxels for Ob-Servo Sanguis irradiator dose mapping [26]. The minor variations could be attributed to measurement uncertainties and approximations used in irradiation modelling. The advantages of Monte Carlo simulations include the ability to supply values anywhere that explain a very tiny peak inside the source rack. Surfer used interpolation with the kriging method to create the curve for the measured absorbed dose rate. This method has a limitation: it cannot estimate precisely inside the source rack, which is why there is a large peak. The discrepancy increased inside the protective cylinder and further out from the conveyor's centre rail due to a lack of experimental data in these places [14]. The relative error was calculated as a means of comparing the data and the Monte Carlo simulation. The relative error values for the absorbed dose rate distribution on center points (radius 7.5 cm and height 10 cm from bottom) are displayed in Tables 3 and 4. With varying target doses, the values range from 1%-3%. Can assume that the Monte Carlo model predicts the absorbed dose rate with a good degree of accuracy based on the very low relative error numbers. As a result, the model is verified through measurements [14].

CONCLUSION

The Gamma Cell 220 model for dosage mapping was implemented using the PHITS algorithm. The doses were measured using an alanine dosimeter. The simulated and measured absorbed

dosage rates were compared. The relative dosage difference was observed to be 2.25%. This is a better result than other previous research, which achieved 10%. In addition, dosage mapping on the XY and Z axes was used to estimate the uniform position in the irradiation chamber. Dose mapping was done using Monte Carlo, and the results were thought to be valid. The results revealed that the relatively small area between 7.5 cm and 12.5 cm on the Z axis from the bottom is the most homogeneous. It should be noted that the area has a radius of no more than 5 cm. In the future, this model can be used for further investigations, such as optimizing the arrangement of 60Co pencils in this irradiator. The irradiation chamber was rearranged to improve radiation results and homogeneity. Dose mapping evaluations will be conducted using a surrogate homogeneous product, and numerous scenarios for reloading the source rack will be investigated.

Improving the discrepancies between the dosage observed and calculated with the Monte-Carlo simulation can be accomplished by detailed component identification and accurate dosimeter calibration. Based on the results, the geometry of the Monte-Carlo simulation is being adjusted to take into account material structures in the gamma irradiators. The inconsistencies are caused by a small number of dosimeters that were slightly inaccurately placed at critical places during the measuring process. The results of the relative difference measurement will be improved by using the proper holder and phantom.

ACKNOWLEDGMENTS

Great appreciations for University of Indonesia, National Research and Innovation Agency (BRIN) and International Atomic Energy Agency (IAEA) Technical Cooperation Programme TC National 5045 Strengthening Food Security through the Improvement of Food Safety for Exports using Gamma Irradiators and Electron Beams for support this project.

REFERENCES

1 Rezaeian, P., Ataenia, V., & Shafiei, S. 2017. An analytical method based on multipole moment expansion to calculate the flux distribution in Gammacell-220. *Radiation Physics and Chemistry, 141*, 339–345.
2 “2020 Optimizing Gamma Irradiation Process”. 2020.
3 Aknouch, A., Elouardi, Y., Mouhib, M., Sebihi, R., Didi, A., & Choukri, A. 2021. A Monte Carlo study to investigate the feasibility to use the Moroccan panoramic irradiator in sterile insect technique programs. *Radiation and Environmental Biophysics, 60*(4), 673–679.
4 Hartmann, G. H., & Andreo, P. 2019. Fluence calculation methods in Monte Carlo dosimetry simulations. *Zeitschrift für Medizinische Physik, 29*(3), 239–248.
5 Hefue, J. 2000. The dose distribution inside the irradiation chamber of the gamma cell 220 at KACST using MCNP4B. *Journal of Nuclear Science and Technology, 37*, 402–405.
6 Gonçalves, J. A. C., Mangiarotti, A., & Bueno, C. C. 2022. Dose rate mapping of an industrial 60Co irradiator using an online photodiode-based dosimetry system. *Radiation Physics and Chemistry, 200*.
7 Sterilization of health care products—Radiation—Part 3: Guidance on dosimetric aspects of development, validation, and routine control. 2017. *ISO*. Online: www.iso.org
8 Eychenne, L., Abdelli-Messaci, S., Trompier, F., Brousse, N., & Achour, S. 2022. High energy X-ray fruit irradiation qualification with Monte Carlo code. *Radiation Physics and Chemistry, 195*.
9 Majer, M., Knežević, Ž., Pasariček, L., & Šarolić, A. 2019. Dose mapping of the panoramic 60Co gamma irradiation facility at the Ruđer Bošković Institute—Geant4 simulation and measurements. *Applied Radiation and Isotopes, 154*.

10 McEvoy, B., Morgan, A., Ferris, R., & Olabisi, O. 2023. Studies on the comparative effectiveness of X-rays, gamma rays, and electron beams to inactivate microorganisms at different dose rates in industrial sterilization of medical devices. *Radiation Physics and Chemistry*.
11 Salehi, Z., Balvasi, E., Zahri, M., & Aziz, A. 2018. A review of the recent Monte Carlo (MC) simulation for dosimetry in mammographic applications.
12 Majer, M., Pasariček, L., & Knežević, Ž. 2024. Dose mapping of the 60Co gamma irradiation facility and a real irradiated product—Measurements and Monte Carlo simulation. *Radiation Physics and Chemistry, 214*.
13 Saputro, B. 2021. Intercomparison of Gamma Cell 220 irradiator facilities and Dr. Mirzan T Razzak gamma irradiators using Harwell dosimeters. *Jurnal Forum Nuklir, 15*(1), 13.
14 Dridi, W., Daoudi, M., Farah, K., & Hosni, F. 2020. Monte Carlo validation of dose mapping for the Tunisian Gamma Irradiation Facility using the MCNP6 code. *Radiation Physics and Chemistry, 173*.
15 Aknouch, A., Elouardi, Y., Mouhib, M., Sebihi, R., Didi, A., & Choukri, A. 2020. New approach to make cylindrical packaging products rotate around their fixed axis during irradiation in the Monte Carlo simulation. *Moscow University Physics Bulletin, 75*(5), 447–450.
16 Peivaste, I., & Alahyarizadeh, G. 2019. Comparative study on absorbed dose distribution of potato and onion in X-ray and electron beam system by MCNPX2.6 code. *MAPAN – Journal of Metrology Society of India, 34*(1), 19–29.
17 Sihver, L., Niita, K., Iwase, H., & Sato, T. 2010. An update about recent developments of the PHITS code. *Advances in Space Research, 45*(7), 892–899.
18 Furuta, T., & Sato, T. 2021. Medical application of particle and heavy ion transport code system PHITS. In *Advances in Radiation Physics* (pp. 67–89). *Springer*.
19 Ladeira, L. C. D., Mesquita, A. Z., & Pereira, M. T. 2015. Calibrations of red Perspex PMMA dosimeter in terms of absorbed dose to water for routine dosimetry at CDTN gamma irradiation laboratory. *International Journal of Nuclear Energy Science and Technology, 9*(3), 238–248.
20 McEwen, M., Miller, A., Pazos, I., & Sharpe, P. 2020. Determination of a consensus scaling factor to convert a Co-60-based alanine dose reading to yield the dose delivered in a high energy electron beam. *Radiation Physics and Chemistry, 171*.
21 Hjørringgaard, J. G., Ankjærgaard, C., Bailey, M., & Miller, A. 2020. Alanine pellet dosimeter efficiency in a 40 kV X-ray beam relative to cobalt-60. *Radiation Measurements, 136*.
22 Nanez, S., & Uribe, R. M. 2023. Performance of the Harwell tape-tab alanine EPR dosimeter under typical production conditions: Effect of irradiation and storage temperature on stability. *Radiation Physics and Chemistry, 206*.
23 Sharpe, P., & Miller, A. 2009. Guidelines for the calibration of routine dosimetry systems for use in radiation processing.
24 Ranković, B. M., Nikolić, N. R., Mašić, S. B., & Vujčić, I. T. 2020. Dose mapping of products with different densities irradiated in 60Co irradiation facility of the Vinča Institute, Serbia. *Nuclear Technology and Radiation Protection, 35*(1), 56–63.
25 Mortuza, M. F., Lepore, L., Khedkar, K., Thangam, S., Nahar, A., Jamil, H. M., ... & Alam, M. K. 2018. Commissioning dosimetry and in situ dose mapping of a semi-industrial Cobalt-60 gamma-irradiation facility using Fricke and Ceric-cerous dosimetry system and comparison with Monte Carlo simulation data. *Radiation Physics and Chemistry, 144*, 256-264.
26 Jecong, J. F. M., Hila, F. C., Pares, F. A., Dingle, C. A. M., Guillermo, N. R. D., Baule, A. G., & Solomon, H. M. 2022. Ob-Servo Sanguis irradiator dose mapping at the Philippine Nuclear Research Institute using MCNP5 annular ring voxels. *Radiation Physics and Chemistry, 191*, 109835.
27 Gual, M. R., Pereira, C., & Mesquita, A. Z. 2019. Application of a new source model of a panoramic gamma irradiator on dose map formation in an irradiated product. *Applied Radiation and Isotopes, 144*, 87–92.
28 Moradi, F., et al. 2021. Feasibility study of a minibeam collimator design for a 60Co gamma irradiator. *Radiation Physics and Chemistry, 178*.
29 Oliveira, C., & Salgado, J. 2001. Isodose distributions and dose uniformity in the Portuguese gamma irradiation facility calculated using the MCNP code.

30 Mannai, K., Askri, B., Loussaief, A., & Trabelsi, A. 2007. Evaluation using Geant4 of the transit dose in the Tunisian gamma irradiator for insect sterilization. *Applied radiation and isotopes*, *65*(6), 701-707.
31 George, J. R., & Pradhan, A. S. 2009. Estimation of DUR and source utilization efficiency for changing product dimensions and source activities in gamma irradiator. *Radiation Physics and Chemistry*, *78*(11), 1011–1014.